Polymer 50 (2009) 3361–3369

Contents lists available at ScienceDirect

Polymer

journal homepage: www.elsevier.com/locate/polymer

Janus-like polymer particles prepared via internal phase separation from emulsified polymer/oil droplets

Yi Wang [a], Bao-Hua Guo [a,*], Xian Wan [a], Jun Xu [a,*], Xin Wang [b], Yin-Ping Zhang [b]

[a] Advanced Materials Laboratory, Department of Chemical Engineering, Tsinghua University, Beijing 100084, PR China
[b] Department of Building Science, Tsinghua University, Beijing 100084, PR China

ARTICLE INFO

Article history:
Received 7 June 2008
Received in revised form
19 February 2009
Accepted 17 March 2009
Available online 3 May 2009

Keywords:
Microparticle
Internal phase separation
Interfacial tension

ABSTRACT

Poly(methylmethacrylate) (PMMA) and polystyrene(PS)/PMMA particles with Janus-like morphology were prepared via the internal phase separation followed by extraction of hexadecane (HD) template. The internal phase separation was triggered by evaporation of dichloromethane (DCM) from the polymer/HD/DCM-in-water emulsion droplets, which led to the formation of HD/PMMA or HD/PMMA/PS microparticles. After extraction of HD with hexane, PMMA or PS/PMMA particles with different morphologies were produced. Poly(vinyl pyrrolidone) (PVP), sodium dodecyl sulfonate (SDS) or sodium dodecyl benzylsulfate (SDBS) was chosen as the emulsifier. The morphology depended on the HD/polymer ratio and the interfacial tensions, which were adjusted by changing the type of the emulsifier and its concentration. With poly(vinyl pyrrolidone) (PVP) emulsifier, PMMA hollow spheres were observed; while with SDS emulsifier, the particles changed from bowl-like particles to hemispheres and truncated spheres with the increase of SDS content. The morphology of PS/PMMA composite particles depended on the ratio of the two polymers. Scanning electron microscopy observation, selective etching and X-ray photoelectron spectroscopy results confirmed that PMMA tended to engulf PS component. With the increase of PMMA/PS ratio, the particles changed the morphology from capped acorn to 'ball in bowl' morphology. Furthermore, the particle morphology was simulated via a theoretical model based on the minimum interfacial energy of the system. The simulation results agreed with the experimental observations. Our results indicate that internal phase separation is an effective method to obtain Janus-like microparticles. Via adjusting the composition of the system and the corresponding interfacial tensions, we could tailor the polymer particles with different morphologies.

1. Introduction

In recent years, polymer particles with different morphologies are of great interest to a wide range of applications including pharmaceuticals, printing, perfumery, cosmetics, and agrochemicals [1–3]. Various methods have been developed, such as seeded polymerization [4–6], interfacial polycondensation [7,8], coaxial jet extrusion [9], Shirasu porous glass (SPG) monomer emulsification accompanied by batch or continuous polymerization [10,11], synthesis in microfluidic reactors [12–14], the electrochemical generation of conducting-polymer microcontainers [15], etc. Besides the aforementioned chemical routes, physical methods have been adopted as well, such as internal phase separation [16–19], coacervation [20,21] and layer-by-layer assembly [22,23].

Among the aforementioned methods, internal phase separation is applicable to most polymers and can be utilized to produce particles in large scale. In this method, the polymer is dissolved in a solvent mixture comprising a volatile solvent and an involatile nonsolvent. A sufficient volume of good solvent is present to ensure that the polymer is (just) dissolved. This solution is then dispersed into a water/emulsifier mixture to produce an oil-in-water emulsion. Evaporation of the volatile solvent leads to a change in the droplet composition, and finally the polymer-rich phase separates as small droplets within the emulsion droplets. The polymer-rich droplets then migrate to the oil/water interface, where they coalesce to form polymer particles. Morphology of the microparticles has been shown to be determined by the thermodynamics, namely, to assure the minimum total interfacial free energy [24–29]. Torza and Mason [24] investigated the equilibrium morphology of the droplets in the system consisted of three immiscible liquids. Depending on the value of the spreading coefficients, core–shell, acorn or separated droplets could be obtained. Loxley and Vincent reported the preparation of poly(methylmethacrylate) (PMMA)

* Corresponding authors. Tel./fax: +86 10 62784550.
E-mail addresses: bhguo@tsinghua.edu.cn (B.-H. Guo), jun-xu@tsinghua.edu.cn (J. Xu).

0032-3861/$ – see front matter © 2009 Elsevier Ltd. All rights reserved.
doi:10.1016/j.polymer.2009.03.061

microcapsules with liquid oil cores using the polymer emulsifiers and acorn particles using the small ionic surfactants [16]. Lavergne et al. [25] produced PMMA microcapsules with foamed membranes via the solvent evaporation technique and revealed that the holes resulted from the encapsulated tiny water droplets in the polymer phase. Composite particles consisted of two polymer components have also been produced, via seed dispersion polymerization (polymerization of a second monomers around the seed particles) [26] or phase separation after evaporation of the co-solvent. In the latter method, when toluene was used as solvent, dimple, acorn or spherical PS/PMMA composite particles could be produced, depending on the surfactant content [27–29].

In the previous reports, core–shell particles with polymer shell and oil core have been produced via internal phase separation [16,19]. In this article, we utilize this method to produce Janus-like polymer particles after extraction of oil. Here, hexadecane plays a role as the sacrifice template. The effect of the emulsifier type and its concentration on the morphology of PMMA particles and the effect of polymer ratio on the PMMA/PS composite particles were investigated. Furthermore, theoretical simulations were carried out to interpret the experimental results.

2. Experimental

2.1. Materials

Methylmethacrylate (MMA, Beijing Yili Fine Chemicals Co., Ltd., 99%) was distilled under vacuum prior to use. The polymerization solvent was THF (Beijing Modern Oriental Fine Chemicals Co., Ltd., 99%) and azobisisobutyronitrile (AIBN, Shanghai No. 4 Reagent & H. V. Chemical Co., Ltd., 97%) was used as the initiator after recrystallization. Hexadecane (HD, Alfa Aesar, 99%) was used as the oil phase. Dichloromethane (DCM, Beijing Beihua Fine Chemicals Co., Ltd., 99%) was used as solvent for both polymer and hexadecane. The emulsifiers used were sodium dodecyl sulfonate (SDS, Shanghai Chemicals Factory, 99%), sodium dodecyl benzylsulfate (SDBS, Shanghai Guanghua Scientific Co., Ltd., 99%) and poly(vinyl pyrrolidone) (PVP, K30, average molecular weight 25,000–40,000, Guangzhou Chemicals Factory, 99%). Polystyrene (PS, 666D, Mn 103,000 and Mw 251,000, Yanshan Petro-Chemical Division, China Petro-Chem Co., Ltd, industrial product) was employed together with PMMA to produce composite particles.

PMMA was synthesized via free-radical solution polymerization according to the method reported in literature [16]. 89 g MMA and 269 g THF were added into a three-neck round-bottomed flask equipped with a paddle agitator, reflux condenser, and nitrogen gas inlet, stirred at 70 °C (controlled by a thermostat water bath) under nitrogen for 30 min. After addition of 0.45 g initiator (AIBN), which was solved in 1 g THF, the polymerization started. After polymerization at 70 °C for 21 hours, PMMA was precipitated via slowly pouring the polymerized solution into a four-fold excess of ethanol, with stirring. After filtration and vacuum drying for overnight, white PMMA powder was obtained. Mn and Mw of the PMMA product were 64,000 and 119,000, respectively.

2.2. Preparation of the microparticles

The internal phase separation method was applied to produce microparticles. First, an o/w emulsion was prepared, which contained, as the oil phase, a mixture of 2.00 g PMMA, 3.00 g incompatible liquid hexadecane (HD), and 80.00 g co-solvent dichloromethane (DCM). The relative amount of DCM was enough for polymer and oil to dissolve in it so that the system was in the one-phase region of the ternary phase diagram, and well away from the phase boundary. The ternary phase diagram had been determined by Loxley and Vincent [16]. DCM is selected due to the low boiling temperature (39 °C) convenient for removing. 0.30 g PVP or SDS was employed as emulsifier in the 200 mL aqueous phase. The oil-in-water emulsion was formed by high-speed shear stirring (5000 rpm) while adding the oil into the aqueous phase. The emulsion was then heated at 40 °C which is the boiling point of DCM in a thermostatted water bath to volatilize DCM from the droplets. When the oil phase composition reached the phase separation point, the polymer phase separated as small droplets of liquid that were rich in DCM and PMMA (called a coacervate phase) within the emulsion droplets. These coacervate droplets were mobile and migrated to the oil/water interface where they fused and grew depending on the interfacial tensions. Twelve hours later, the emulsion was subjected to vacuum (1 kPa) so as to remove all the residual DCM in the droplets, causing the PMMA to precipitate and solidify at the interface. Eventually, the PMMA particles were obtained after extracting HD with n-hexane and drying. Different emulsifiers were used to change the particle morphology.

To prepare composite polymer particles, the blends of PS and PMMA with different weight ratios were employed as the polymer matrix via the aforementioned procedures except that 0.125% sodium dodecyl benzylsulfate (SDBS) was used as emulsifier. The weight ratio of Polymer/HD/CH_2Cl_2 was fixed at 2/3/80.

2.3. Characterization

Interfacial tensions between the polymer and the various aqueous phases were determined by measuring the contact angle of each liquid against the films of PMMA or PS, which were prepared via hot press. Contact angles were measured using a home-made equipment. At least seven measurements were made for each liquid–polymer pair, and the mean contact angle was used to calculate the solid–liquid interfacial tension.

The separation process in the emulsion system was monitored by a phase contrast microscope (BH-2, Olympus) coupled with a computer controlled CCD-camera (Sanyo Electric Co., Ltd.).

The polymer particles were washed three times with deionized water to remove the surfactant. After that, the dispersion of polymer particles was dropped onto a clean silicon wafer and dried in a hot oven for overnight. The particles were observed directly under scanning electron microscope (JSM 7401, JEOL, Japan) with an accelerating electronic voltage of 1 kV.

X-ray photoelectron spectroscopy (XPS) spectra of the particles were collected in a Physical Electronics ESCA PHI 5300 spectrometer (Perkin–Elmer, USA). Mg Kα X-ray (1253.6 eV, 250 W) was used to induce electron ejection from the samples. The photoelectrons were collected at a pass energy of 50 eV and a step size of 50 eV. The pressure in the sample chamber was kept below 10^{-6} Pa. The charging of the samples, due to photoemission, was corrected by setting the binding energy of the main hydrocarbon component of C_{1S} spectra at 285.0 eV. Curve fitting of the spectra was done using a combination of Gaussian and Lorentzian peak shapes.

3. Results

3.1. Production of PMMA particles via internal phase separation

The scheme of the internal phase separation method used here is shown in Fig. 1, redrawn from literature [16]. Evaporation of DCM triggered the internal phase separation in the polymer/HD/DCM droplets. When PVP was used as the emulsifier, the core–shell microcapsules with PMMA shell encapsulating the HD core were produced. After extraction of HD with hexane, the hollow PMMA spheres were obtained (Fig. 2a). Collapse was observed on the surface of some spheres, which could probably be attributed to the

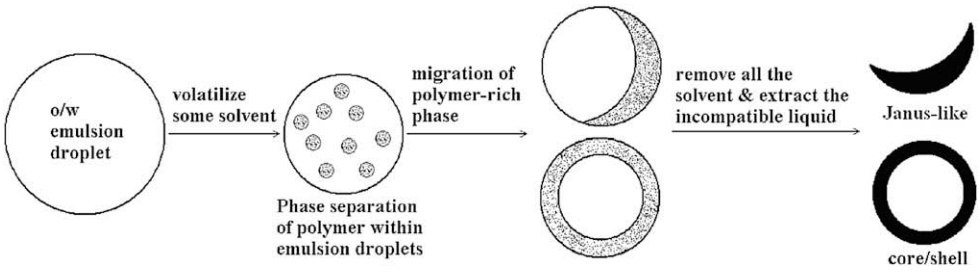

Fig. 1. Scheme of the internal phase separation in the PMMA/hexadecane/CH_2Cl_2/aqueous phase system.

buckling caused by extraction of HD or vacuum drying [16]. Diameter of the hollow spheres was in the range of 0.5–6 μm, most of which lied in 1–3 μm range. From the fractured capsules in Fig. 2a, the shell thickness was estimated to around 0.1–0.3 μm. Variation of PVP concentration from 0.15% to 0.5% did not change the morphology of the microcapsules.

When SDS was employed as emulsifier, Janus-like particles were prepared. The results agree with Loxley and Vincent's observation that the PMMA/HD/CH_2Cl_2 system adopted acorn morphology during evaporation of CH_2Cl_2 [16]. However, the authors did not report the effect of SDS concentration on the microparticle morphology. In this study, we observed that the SDS concentration had considerable effect on the PMMA microparticle morphology, as shown in Fig. 2b–d. At the lowest SDS content of 0.05%, the bowl-like microparticles were obtained (Fig. 2b). Diameter of the "bowls" ranged from 0.1 to 0.5 μm. They are totally different from the collapsed capsules during SEM preparation observed by Loxley and Vincent (Fig. 10c and Fig. 13a in literature [16]). There were cracks on the surface of the collapsed capsules. In addition, there were also some intact capsules. In our case, all the particles, whether big or small, are of bowl shape and the surface is smooth. With further increase of SDS concentration to 0.1%, hemisphere particles were produced (Fig. 2c). When SDS content reached 0.25%, truncated spheres were observed (Fig. 2d). With further increase of SDS content to 0.5% and 1%, the morphology of the microparticles did not change anymore. It suggests that with the increase of SDS content the tendency of the PMMA shell engulfing the incompatible oil HD is reducing, namely HD is getting out from the engulfment of the PMMA shell. This is probably due to the reduction of the surface tension of the aqueous phase with increasing emulsifier concentration, inducing the HD phase to contact with the aqueous phase instead of the polymer-rich phase. The critical micelle concentration of SDS is 8 mmol/L at 20 °C, namely 0.22 wt%. When SDS amount is larger than the value it will not affect the surface tension of the aqueous phase anymore, thus the morphology of the final PMMA microparticles will not change anymore.

The phase separation structures in the droplets were not formed until partial evaporation of the co-solvent occurred, as shown by

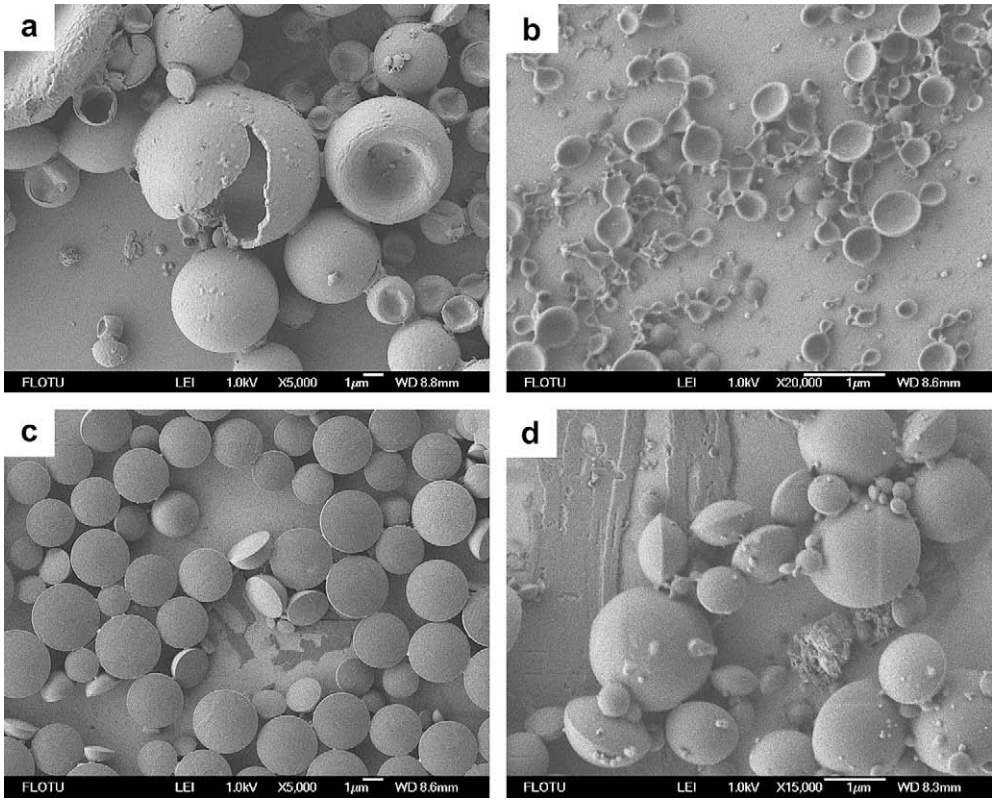

Fig. 2. SEM micrographs of the PMMA particles obtained from various emulsifiers in the aqueous phase: (a). 0.5% PVP (b). 0.05% SDS; (c). 0.1% SDS; (d) 0.25% SDS.

the phase contrast microscopy observation. Before heated at 40 °C, the emulsion droplets were homogeneous (Fig. 3a). After heating for about 12 hours, most DCM had been volatilized and an "acorn"-like two-phase structure was formed due to the internal phase separation (Fig. 3b). The experimental conditions are the same as those in Fig. 2d with the SDS content of 0.25%. The particle morphology in Fig. 3b is similar to that reported by Loxley and Vincent [16]. The oil/polymer ratio used by them was 1.5, the same as ours. The only difference is the SDS content, which was 1% in literature [16] and 0.25% in this article. The comparison agrees with our previous statement that the SDS content has little effect on the particle morphology when it is much larger than the critical micelle concentration, 0.22%.

The process of the internal phase separation can be described as follows: with the volatilization of the co-solvent, the oil phase composition moved from the one-phase region to the two-phase region. As a result, PMMA-rich phase was separated in the emulsion droplet in the form of tiny droplets. Each emulsion droplet was comprised of two phases, the oil phase and the polymer-rich phase. During the further evaporation process of DCM, the tiny droplets of polymer-rich phase migrated to the surface of the emulsion droplets, and coalesced there to form the microparticles. The three-phase interaction induced by the interfacial tensions was the primary driving force for the migration of the polymer-rich phase, and it affected the degree of spreading of the polymer-rich phase on the surface of the emulsion droplets. Therefore, the interfacial tensions determined the final equilibrium morphology of the phase-separated droplets. After all the co-solvents were removed, the polymer phase was solidified and the shapes of the particles did not change anymore. The structure of the obtained polymer particles is determined by the interfacial tensions between the oil phase, the polymer phase and the aqueous phase containing the emulsifier. Based on this, we can obtain polymer microparticles with the controlled structures by employing different emulsifiers or different amounts of emulsifier.

3.2. Production of PS/PMMA composite particles via internal phase separation

To produce composite polymer particles, we selected PMMA and PS, which have different interface tensions with oil and aqueous phases but both soluble in the co-solvent CH_2Cl_2. The total weight of the two polymers was fixed, but with different PS/PMMA ratios. After the internal phase separation due to CH_2Cl_2 evaporation and thereafter extraction of HD with hexane, PS/PMMA composite particles with novel morphologies were produced. For pure PS, the microspheres with diameter of 1–6 μm were obtained (Fig. 4a). For PS/PMMA 75/25 blend, the particles with small caps were produced (Fig. 4b). When PS/PMMA ratio was decreased to 50/50 and 33/67, "ball in bowl" morphology was observed (Fig. 4c and d). With a further decrease of PS, the composite particles with a dimple were formed (Fig. 4e). On the basis of the increased fraction of the encapsulating component, we suggest that PMMA tends to engulf PS component. For pure PMMA, the particles were truncated spheres rather than the whole spheres (Fig. 4f).

To distinguish the two parts of the "ball in bowl" particles, we washed them twice with styrene to remove the PS component. After washing, the ball part was removed and the bowls were left (Fig. 5), which demonstrates that the ball and the bowl parts consist of PS and PMMA, respectively. The conclusion is further confirmed by the element analysis of the content of C and O atoms in the particles via XPS. Before styrene washing, the C/O ratio of the "ball in bowl" particles is 4.85, which agrees with the theoretical result calculated from the feed ratio of PS/PMMA (Table 1). After washing with styrene, the bowl-shaped particles have a decreased C/O ratio 1.93, which is very close to the theoretical value in pure PMMA. Consequently, styrene washing leads to almost complete dissolution of the PS part. All the experimental results reveal that in the PS/PMMA composite particles PMMA tends to engulf PS.

The formation mechanism of the PS/PMMA composite particles is schemed in Fig. 6. The phase separation in the PS/PMMA/HD/CH_2Cl_2 droplets is expected to be more complicated than that occurred in the previously reported PMMA//HD/CH_2Cl_2 droplets. With evaporation of CH_2Cl_2, phase separation of the former may lead to formation of three phases: PS rich, PMMA rich and HD rich phases; while that of the latter leads to formation of only two phases: PMMA rich and HD rich phases. The contact angle of SDBS solution on PMMA and PS was determined to be 39° and 41°, respectively. The surface tension of 0.125% SDBS is 34 mN m^{-1} [30]. The surface tension of bulk PMMA and PS is 41.1 and 40.7 mN m^{-1}, respectively [31]. The interfacial tension between PMMA and the aqueous phases is calculated to be 14.7 mN m^{-1}, which is smaller than that between PS and aqueous phases, 15.0 mN m^{-1}. As a result, the PMMA engulfing PS morphology has the lower total interfacial energy than the opposite.

The PS/PMMA composite particles reported here using CH_2Cl_2 as co-solvent and hexadecane oil as template have different morphologies from those obtained by Saito et al. using styrene as the co-solvent without the oil phase [28,29]. In the latter case, the obtained composite particles were acorns, spheres or spheres with

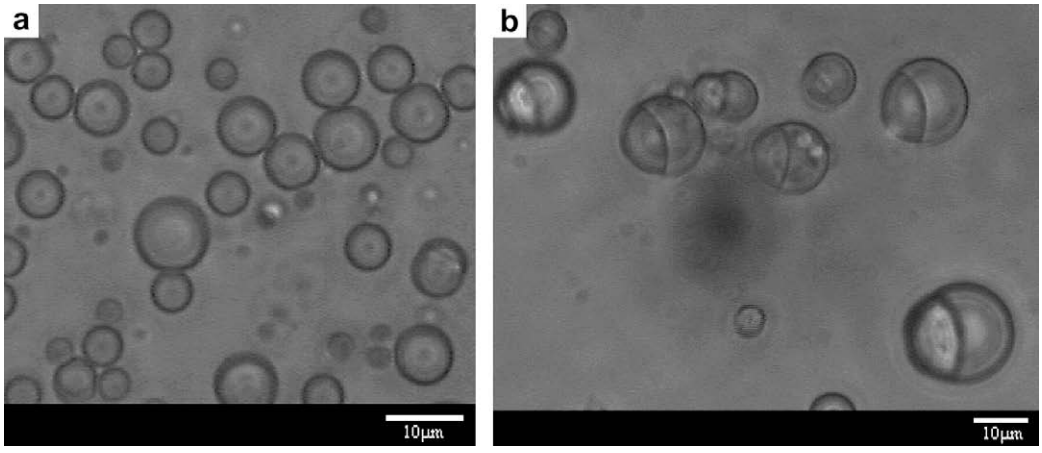

Fig. 3. Optical micrographs of emulsion droplets: (a) before evaporation of dichloromethane; (b) after heating at 40 °C for 12 hours.

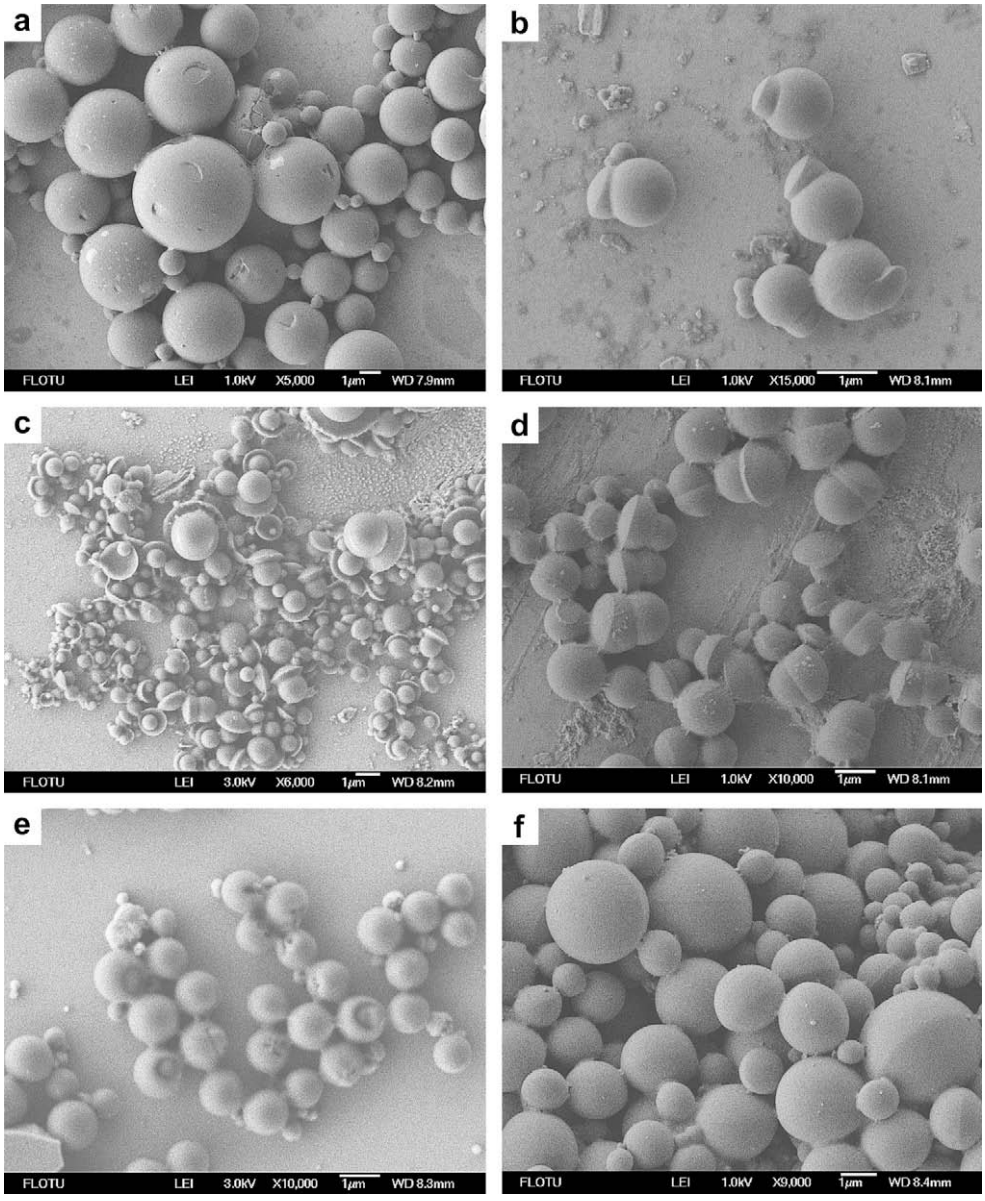

Fig. 4. SEM micrographs of the PS/PMMA composite particles obtained from various PS/PMMA ratios: (a). 100/0; (b). 75/25; (c). 50/50; (d) 33/67; (e)25/75; (f) 0/100.

dimple. We attribute the morphology difference predominantly to the effect of the hexadecane template, which produces additional interfaces, namely hexadecane–water, hexadecane/PMMA and hexadecane/PS interfaces. After the internal phase separation completes, the hexadecane templates can be easily removed via hexane extraction. Consequently, application of both internal phase separation and a sacrifice template can tune the polymer particle morphology in a wider range.

4. Discussion

To quantitatively explain the change of particle morphology with the type and the concentration of the emulsifier, we have to closely examine the internal phase separation process of the three-phase system. Although in our work the final state was a solid–liquid system, we propose that the equilibrium morphology depends on the interfacial tensions. It has been reported that both thermodynamics and kinetics affect the particle morphology [4,16]. For simplicity, only the thermodynamic effect is taken into account in this article. Gravity, fluid motion and interparticle forces, which may also effect the equilibrium configuration of the system, were not taken into account.

Three interface tensions (σ_{12}, σ_{13}, σ_{23}) were considered, where the subscript 1, 2 and 3 denotes HD phase, aqueous phase and polymer phase, respectively.

4.1. Determination of interfacial tensions (σ_{12}, σ_{13}, σ_{23})

According to Antonoff rule, for two contacting liquids:

$$\sigma_{12} = |\sigma_1 - \sigma_2| \quad (1)$$

σ_1 is the surface tension of oil phase (HD). Its value is 27.5 mN m^{-1} at 20 °C [32].

σ_2 is the surface tension of aqueous phase. When PVP was used as the surfactant, the surface tension of PVP solution decreased from 73 mN m^{-1} to 65 mN m^{-1} with increase of PVP concentration

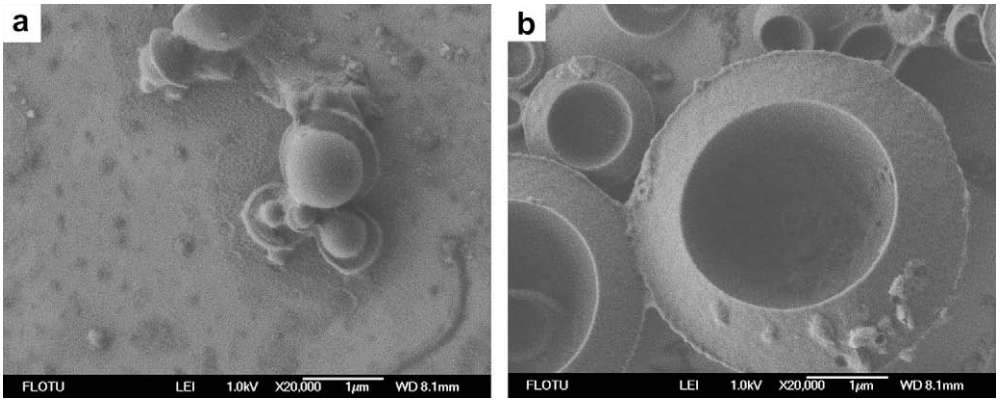

Fig. 5. SEM micrographs of the PS/PMMA composite particles obtained from 50/50 PS/PMMA: (a) before styrene washing; (b) after styrene washing to remove PS part.

Table 1
Content of C and O atoms in the composite PS/PMMA particles.

Sample	C (%)	O (%)	Real C/O ratio	Theoretical C/O ratio
PS/PMMA = 1/1	36.98	7.62	4.853	4.760
PS/PMMA = 1/1 washed by Styrene	24.55	12.73	1.929	1.875

from 0 to 4% [33]. When SDS was used as surfactant, with increase of SDS amount from 0.05% to 0.1% and 0.25%, surface tension of the aqueous phase is decreased from 55 to 43 and 34 mN m^{-1} at 20 °C [31].

σ_3 is the surface tension of PMMA. Its value is 41.1 mN m^{-1} at 20 °C [34].

Substituting the surface tensions into Eq. (1), σ_{12} of different SDS amounts at 20 °C can be calculated (Table 2).

σ_{13} is the interfacial tension between oil phase (HD) and polymer phase (PMMA). This is a constant value at a given temperature. It was calculated to be 14.6 mN m^{-1} at 20 °C based on the data reported in literature [16].

σ_{23} is the interfacial tension between aqueous phase (SDS solution) and polymer phase (PMMA), which is calculated from the measured contact angle. According to Young's equation:

$$\sigma_{23} = \sigma_3 - \sigma_2 \cos\theta_{23} \tag{2}$$

θ_{23} is the contact angle of SDS solution on PMMA, which is shown in Table 2. All the interfacial tensions at 20 °C are listed in Table 2 as well.

4.2. Determination of PMMA particle geometry for PMMA/HD/CH_2Cl_2 system

Fig. 7 defines a number of quantities that describe the shape of a three-phase construction consisting of three spherical segments

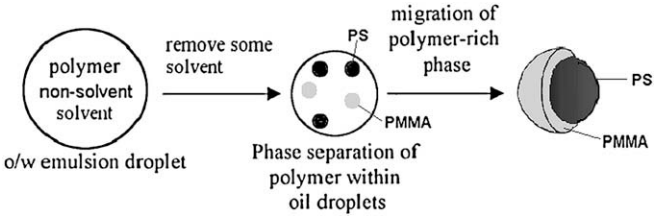

Fig. 6. Scheme of the internal phase separation in the PMMA/PS/hexadecane/CH_2Cl_2/aqueous phase system.

Table 2
Interfacial tensions in the PMMA/oil/aqueous phase system.

Surfactant	Contact angle on PMMA	σ_2 (mN m^{-1})	σ_{12} (mN m^{-1})	σ_{23} (mN m^{-1})	σ_{13} (mN m^{-1})
PVP	70.0	70	42.5	17.1	14.6
0.05% SDS	73.0	55	27.5	25.0	14.6
0.10% SDS	46.7	43	15.5	11.6	14.6
0.25% SDS	43.9	34	6.5	16.6	14.6

with radius of curvature r_{ij}, where 1, 2, 3 stand for HD phase, aqueous phase and polymer phase, respectively.

The volume of HD and polymer is:

$$V_1 = \frac{\pi}{3}\left[r_{12}^3(1-\cos\phi_{12})^2(2+\cos\phi_{12}) \pm r_{13}^3(1-\cos\phi_{13})^2(2+\cos\phi_{13})\right] \tag{3}$$

$$V_3 = \frac{\pi}{3}\left[r_{23}^3(1-\cos\phi_{23})^2(2+\cos\phi_{23}) \mp r_{13}^3(1-\cos\phi_{13})^2(2+\cos\phi_{13})\right] \tag{4}$$

The three interfaces between each phase:

$$S_{12} = 2\pi r_{12}^2(1-\cos\phi_{12}) \tag{5}$$

$$S_{23} = 2\pi r_{23}^2(1-\cos\phi_{23}) \tag{6}$$

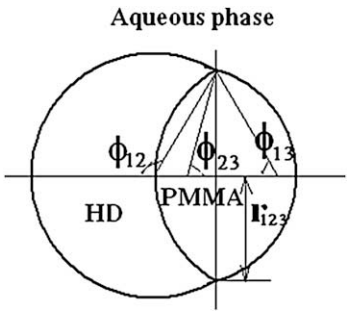

Fig. 7. Configuration of the equilibrium state showing various geometrical parameters of the oil and the polymer phases suspended in the emulsion.

$$S_{13} = 2\pi r_{13}^2(1-\cos\phi_{13}) \tag{7}$$

The total interface free energy:

$$\begin{aligned} G &= \sigma_{12}S_{12}+\sigma_{23}S_{23}+\sigma_{13}S_{13} \\ &= 2\pi\Big[\sigma_{12}r_{12}^2(1-\cos\phi_{12})+\sigma_{23}r_{23}^2(1-\cos\phi_{23}) \\ &\quad +\sigma_{13}r_{13}^2(1-\cos\phi_{13})\Big] \end{aligned} \tag{8}$$

According to the geometry shown in Fig. 4, we have:

$$r_{12}\sin\phi_{12} = r_{23}\sin\phi_{23} = r_{13}\sin\phi_{13} = r_{123} \tag{9}$$

The volume ratio of HD to polymer:

$$M = \frac{V_1}{V_3} = \frac{m_1}{m_3}.\frac{\rho_3}{\rho_1} \tag{10}$$

where $\rho_1 = 0.77$ g/cm^3, $\rho_3 = 1.18$ g/cm^3.

Substituting Eqs. (3), (4) and (9) into Eq. (10), we obtain:

$$\frac{(1-\cos\phi_{12})^2(2+\cos\phi_{12})/\sin^3\phi_{12} \pm (1-\cos\phi_{13})^2(2+\cos\phi_{13})/\sin^3\phi_{13}}{(1-\cos\phi_{23})^2(2+\cos\phi_{23})/\sin^3\phi_{23} \mp (1-\cos\phi_{13})^2(2+\cos\phi_{13})/\sin^3\phi_{13}} = M \tag{11}$$

Substituting Eq. (9) to Eq. (8), it gives:

$$\begin{aligned} G = 2\pi\Bigg[&\sigma_{12}\frac{r_{123}^2}{\sin^2\phi_{12}}(1-\cos\phi_{12})+\sigma_{23}\frac{r_{123}^2}{\sin^2\phi_{23}}(1-\cos\phi_{23}) \\ &+\sigma_{13}\frac{r_{123}^2}{\sin^2\phi_{23}}(1-\cos\phi_{13})\Bigg] \end{aligned} \tag{12}$$

When the system reaches the equilibrium state, the free energy should be at the minimum value, so it gives:

$$G(\Phi_{12},\Phi_{13},\Phi_{23}) = G_{\min} \tag{13}$$

Combining Eqs. (11)–(13), we can get (Φ_{12}, Φ_{13}, Φ_{23}) for known parameters: M, σ_{12}, σ_{13} and σ_{23}. Eq. (13) indicates that the particle geometry is independent of the particles size, which agrees with the previous reports [16,28].

For a system using 3.00 g HD, 2.00 g PMMA and different SDS contents, $M = 2.30$. The volume ratio of the core to the shell component, M, affects the particle geometry. When M is constant, the interfacial tension between the oil and the polymer phases σ_{13} varies little with the surfactant content, so the particle morphology depends only on the normalized interfacial tensions, namely:

$$(\Phi_{12},\Phi_{13},\Phi_{23}) = \mathrm{F}(\sigma_{12}/\sigma_{13},\sigma_{23}/\sigma_{13}) \tag{14}$$

Thus we can draw a geometry map of the oil/polymer particle with variation of the interfacial tensions and the ratio of the two components. The simulated particle geometries with $M = 2.3$ are shown in Fig. 8, depending on the normalized interfacial tension σ_{12}/σ_{13} and σ_{23}/σ_{13}. The map can be divided into four regions:

Region I: When $\sigma_{12}/\sigma_{13}+\sigma_{23}/\sigma_{13} \le 1$, the separated droplets of oil and polymer phases will be obtained from the internal phase separation.

Region II: When $\sigma_{12}/\sigma_{13}-\sigma_{23}/\sigma_{13} \ge 1$, the core–shell particles with phase 1 as core and phase 3 as shell will be produced.

Region III: When $\sigma_{23}/\sigma_{13}-\sigma_{12}/\sigma_{13} \ge 1$, the core–shell particles with phase 3 as core and phase 1 as shell will be expected.

Region IV: When $\sigma_{12}/\sigma_{13}+\sigma_{23}/\sigma_{13} > 1$ and $-1 < \sigma_{12}/\sigma_{13}-\sigma_{23}/\sigma_{13} < 1$, the acorn-shaped particles are the equilibrium morphology. In Region IV, when $\sigma_{12}/\sigma_{13}-\sigma_{23}/\sigma_{13}$ draws near 1, bowl-shaped polymer particles can be produced after the oil is extracted; when $\sigma_{12}/\sigma_{13}-\sigma_{23}/\sigma_{13}$ draws near −1, truncated spheres can be obtained.

The region boundaries are independent of the oil/polymer volume ratio M though M will affect the detailed geometry of the oil/polymer composite particle. The region boundaries given by our model agree with Torza and Mason's criteria [24] based on the spreading coefficients, $S_i = \sigma_{jk}-(\sigma_{ij}+\sigma_{ik})$, $i, j, k = 1, 2, 3$.

In the case of 0.25% SDS, $\sigma_{12} = 6.5$ mN m^{-1}, $\sigma_{13} = 14.6$ mN m^{-1}, $\sigma_{23} = 16.6$ mN m^{-1}. We obtain: $\Phi_{12} = 134°$, $\Phi_{23} = 107°$, $\Phi_{13} = 51°$ (truncated sphere).

In the case of 0.1% SDS, $\Phi_{12} = 132°$, $\Phi_{23} = 113°$, $\Phi_{13} = 3°$ (hemisphere).

In the case of 0.05% SDS, $\Phi_{12} = 119°$, $\Phi_{23} = 92°$, $\Phi_{13} = 3°$ (hemisphere).

The simulated data are in accordance with the experimental results except that in the case of 0.05% SDS. We attribute the discrepancy to underestimation of the surface tension of the aqueous phase containing 0.05% SDS, which was adopted from literature [32]. Since the contact angle data are similar to that of PVP solution on PMMA, the surface tension of 0.05% SDS is estimated in the range of 65–70 mN m^{-1}. Using this surface tension value, the calculated morphology agrees with the observed "bowl shape" morphology.

The effect of PVP as surfactant is very limited. Even when PVP content reaches up to 10 wt%, the surface tension of the aqueous phase decreases only slightly to 65 mN m^{-1}. In the case of PVP surfactant, $\sigma_{12}/\sigma_{13}-\sigma_{23}/\sigma_{13} \ge 1$, the simulated result is core–shell particle with phase 1 (hexadecane) as the core, which agrees with the observed morphology.

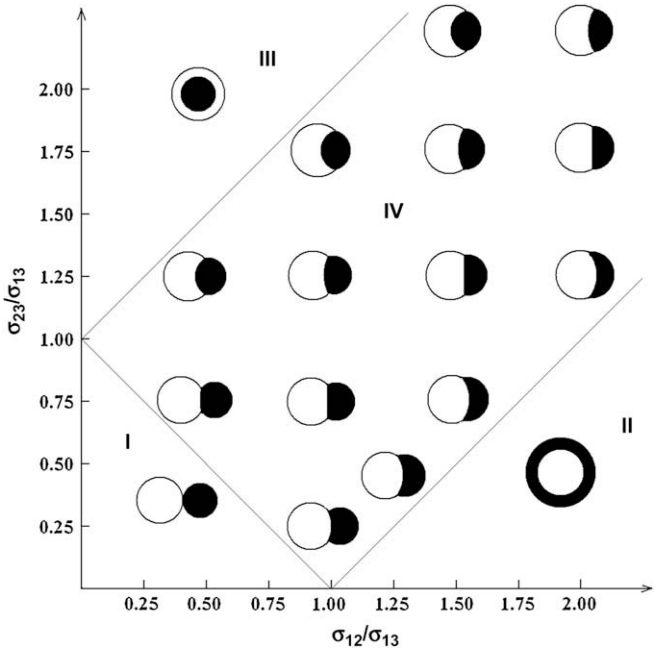

Fig. 8. Simulated morphology of the equilibrium particle depending on the interfacial tensions. The white indicates phase 1 (oil), the black indicates phase 3 (polymer) and the surrounding medium is phase 2 (the aqueous phase). $\sigma_{i,j}$ indicates the interfacial tension between phases i and j. The volume ratio of HD to polymer is fixed at 2.3.

SDS is a more efficient surfactant than PVP. Addition of SDS leads to considerable decrease of the surface tension of the aqueous phase. When SDS content increases from 0.05% to 0.25%, the surface tension of the aqueous solution decreases from 55 to 34 mN m^{-1}(Table 1). In the studied SDS range, the interfacial intensions meet $\sigma_{12}/\sigma_{13}+\sigma_{23}/\sigma_{13}>1$, $-1<\sigma_{12}/\sigma_{13}-\sigma_{23}/\sigma_{13}<1$, or $S_1=\sigma_{23}-(\sigma_{12}+\sigma_{13})<0$, $S_2=\sigma_{13}-(\sigma_{12}+\sigma_{23})<0$ and $S_3=\sigma_{12}-(\sigma_{13}+\sigma_{23})<0$, so the acorn-shaped polymer–hexadecane particles were formed as a result of the phase separation. At the SDS content of 0.05%, $\sigma_{12}>\sigma_{23}$, the phase 3 (PMMA) tends to encapsulate phase 1 (HD), as a result, bowl-like PMMA particles were produced. At the SDS content of 0.25%, $\sigma_{12}<\sigma_{23}$, the phase 1 (HD) tends to encapsulate phase 3 (PMMA), so the truncated PMMA spheres were obtained.

4.3. Determination of PMMA particle geometry for PS/PMMA/HD/CH_2Cl_2 system

The simulation method of oil–PMMA–aqueous phase can be further applied to the four-phase system consisted of oil (phase 1), PMMA (phase 3), PS (phase 4) and the aqueous phase (phase 2) according to the criteria of minimum total interfacial energy. The following interfacial tensions were adopted: $\sigma_{12}=6.5$ mN m^{-1}, $\sigma_{23}=14.7$ mN m^{-1}, $\sigma_{34}=3.2$ mN m^{-1}, $\sigma_{14}=2.2$ mN m^{-1}, $\sigma_{13}=14.6$ mN m^{-1} and $\sigma_{24}=15.0$ mN m^{-1}. In the model, PS particles are complete spheres (demonstrated by the SEM results in Fig. 4). The simulated morphologies of the composite particles are shown in Fig. 9, depending on the weight ratio of PMMA to PS. The simulation results agree well with the experimental observations.

To the best of our knowledge, theoretical modeling of the equilibrium geometry of the composite particles containing three phases has not been carried out. Based on the criteria of minimum interfacial free energy, our model uses the azimuth angles of the phase boundaries as the geometric parameters rather than the detailed size in the previous simulation models. It is mathematically simple and can be easily applied to predict the geometry of three-component composite particles. It should be pointed that phase separation kinetics also has some effects on the geometry of the composite particles, so there are two other factors that should be considered in future research and modeling. The first one is that the oil phase may contain a small amount of polymer and the polymer phase may contain a small amount of oil, which has been noted by Saito et al. [28,29]. The main challenge is how to determine the phase compositions and the interfacial tension between two phases (at least one phase with high viscosity). The second factor is the kinetics effect, namely, during evaporation of CH_2Cl_2, the mobility of polymer/CH_2Cl_2 phase decreases steadily, when CH_2Cl_2 decreases to a certain content, the phase cannot move at all to reach the minimum interfacial energy state. After this stage, the geometry was trapped due to the limited diffusion effect. Later, evaporation of the residual CH_2Cl_2 leads to shrinkage of the polymer phase. Chen et al. have reported the kinetics effect on the morphology of composite PS/PMMA particles produced from MMA polymerization around the PS latex seeds due to the restricted chain mobility related to high internal viscosity during the final stage of the polymerization [4]. It is a pity that this kinetic effect has seldom been considered in geometry prediction of the composite particle produced from internal phase separation. We expect that real-time observation may provide more information on the internal phase separation process. In addition, we expect that further theoretical simulation can take into account the effect of another polymer and residual solvent on the interfacial tensions and the kinetics effect due to steady increase of the viscosity of the polymer-rich phase during the phase separation process.

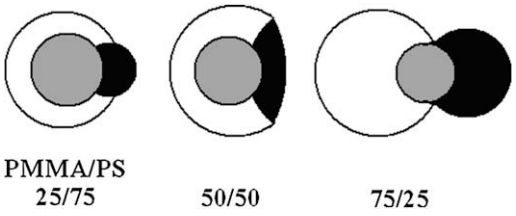

Fig. 9. Simulated morphology of PS/PMMA composite particles via internal phase separation. The white, gray and black components indicate hexadecane oil, PS and PMMA, respectively. The surrounding medium is the aqueous phase containing SDBS.

5. Conclusion

In conclusion, we have demonstrated that PMMA and PS/PMMA composite microparticles with different morphologies could be produced via the internal phase separation from emulsified polymer/hexadecane/dichloromethane droplets in aqueous solution via evaporation of the solvent CH_2Cl_2 and the following extraction of hexadecane via hexane. The type of the emulsifier and its concentration affect the particle morphology. Hollow PMMA spheres were obtained using PVP emulsifier. Janus-like PMMA particles were produced with SDS emulsifier. With increase of the SDS content from 0.05% to 0.25%, the morphology of the particles varied from bowl-shaped to hemisphere and truncated sphere. In addition, PMMA/PS composite particles with "ball in bowl", "capped sphere" and "sphere with a dimple" morphologies were produced via alteration of the PMMA/PS ratio with 0.125% SDBS emulsifier. Two components of the composite particles were identified via selective solvent washing and XPS element analysis. Furthermore, morphology of the PMMA and PS/PMMA composite particles formed from the internal phase separation was simulated. It is demonstrated that the criteria of minimum total interfacial energy could be applied to the internal phase separation in the more complex system. It should be noted that the dynamics of phase separation may have some effects on the particle morphology, which is the focus in future research. The obtained hollow spheres and Janus-like particles may find potential applications in drug delivery, microreactors, immobilized enzyme, phase change materials and other fields as functional material. Comparing to the other methods for preparing microcontainers, such as interfacial polymerization, coacervation and layer-by-layer self-assembly, the internal phase separation method may be applied to most polymers if a suitable co-solvent for the polymer and the incompatible liquid can be found.

Acknowledgment

Financial support from the National Natural Science Foundation of China (No. 50436020, 50673050) is highly appreciated.

References

[1] Xing FB, Cheng GX, Yang BX, Ma LR. J Appl Polym Sci 2004;91:2669–75.
[2] Teshima K. Adv Eng Mater 2003;5:512–4.
[3] Miyazawa K, Yajima I, Kaneda I, Yanaki T. J Cosmet Sci 2000;51:239–52.
[4] Chen YC, Dimonie V, El-Aasser MS. Macromolecules 1991;24:3779–87.
[5] Okubo M, Izumi J, Hosotani T, Yamashita T. Colloid Polym Sci 1997;275:797–801.
[6] Chen YC, Dimonie V, El-Aasser MS. Colloid Polym Sci 2005;283:691–8.
[7] Park SJ, Shin YS, Lee JR. J Colloid Interface Sci 2001;241:502–8.
[8] Jiang YB, Wang DJ, Zhao T. J Appl Polym Sci 2007;104:2799–806.
[9] Berkland C, Pollauf E, Varde N, Pack DW, Kim K. Pharm Res 2007;24:1007–13.
[10] Chu LY, Xie R, Zhu JH, Chen WM, Yamaguchi T, Nakao S. J Colloid Interface Sci 2003;265:187–96.
[11] Liu R, Ma GH, Meng FT, Su ZG. J Controlled Release 2005;103:31–43.

[12] Xu S, Nie ZH, Seo M, Lewis P, Kumacheva E, Stone HA, et al. Angew Chem Int Ed 2005;44:724–8.
[13] Dendukuri D, Tsoi K, Hatton TA, Doyle PS. Langmuir 2005;21:2113–6.
[14] Nie ZH, Xu SQ, Seo M, Lewis PC, Kumacheva E. J Am Chem Soc 2005;127:8058–63.
[15] Qu LT, Shi GQ, Chen FE, Zhang JX. Macromolecules 2003;36:1063–7.
[16] Loxley A, Vincent B. J Colloid Interface Sci 1998;208:49–62.
[17] Shulkin A, Stöver HDH. Macromolecules 2003;36:9836–9.
[18] Atkin R, Davies P, Hardy J, Vincent B. Macromolecules 2004;37:7979–85.
[19] Dowding PJ, Atkin R, Vincent B, Bouillot P. Langmuir 2004;20:11374–9.
[20] Nakagawa K, Iwamoto S, Nakajima M, Shono A, Satoh K. J Colloid Interface Sci 2004;278:198–205.
[21] Quek CH, Li J, Sun T, Ling M, Chan H, Mao HQ, et al. Biomaterials 2004;25:3531–40.
[22] Zhang YJ, Guan Y, Yang SG, Xu J, Han CC. Adv Mater 2003;15:832–5.
[23] Peyratout CS, Dähne L. Angew Chem Int Ed 2004;43:3762–83.
[24] Torza S, Mason SG. J Colloid Interface Sci 1970;33:67–83.
[25] Lavergne FM, Cot D, Ganachaud F. Langmuir 2007;23:6744–53.
[26] Sundberg DC, Durant YG. Polym React Eng 2003;11:379–432.
[27] Okubo M, Saito N, Fujibayashi T. Colloid Polym Sci 2005;283:691–8.
[28] Saito N, Kagari Y, Okubo M. Langmuir 2006;22:9397–402.
[29] Saito N, Kagari Y, Okubo M. Langmuir 2007;23:5914–9.
[30] Flaming JE, Knox RC, Sabatini DA, Kibbey TC. Vadose Zone J 2003;2:168–76.
[31] Rana D, Neale GH, Hornof V. Colloid Polym Sci 2002;280:775–8.
[32] http://www.surface-tension.de.
[33] Lee DY, Kim BY, Lee SJ, Lee MH, Song YS, Lee JY. J Korean Phys Soc 2006;48:1686–90.
[34] http://www.surface-tension.de/solid-surface-energy.htm.